Contents lists available at ScienceDirect

Transactions of Nonferrous Metals Society of China

36(2026) 273−286

www.tnmsc.cn

Adsorption properties of ammonium dibutyl dithiophosphate on argentite and sphalerite surface in pulp containing silver and zinc ions

Ting-sheng QIU [a,b], Kai-wei DING [a,b], Guan-fei ZHAO [a,b,*], Guo-dong LI [a,c,**], Wen-hui YANG [a,b], Hao CHENG [a,b], Shun-de YAN [a,b]

[a] Jiangxi Provincial Key Laboratory of Low-Carbon Processing and Utilization of Strategic Metal Mineral Resources, Jiangxi University of Science and Technology, Ganzhou 341000, China;

[b] School of Resources and Environmental Engineering, Jiangxi University of Science and Technology, Ganzhou 341000, China;

[c] Northwest Research Institute of Mining and Metallurgy, Baiyin 730900, China

Abstract: The flotation separation of argentite from sphalerite using ammonium dibutyl dithiophosphate (ADD) was studied. Molecular simulation (MS) calculation shows that ADD is chemisorbed on argentite and sphalerite surface in the form of S—P bond. The ADD adsorption on argentite and sphalerite surface in Ag^+ system was revealed by ICP, Zeta potential and XPS analyses. It is shown that the dissolved Ag^+ from argentite surface can be absorbed on sphalerite surface in the form of silver hydroxide, and AgOH hydrophilic colloid prevents the adsorption of ADD on sphalerite surface. The ADD adsorption on argentite and sphalerite surface in the pulp containing silver and zinc ions was revealed by adsorption capacity and surface wettability analyses. It is shown that the combined $Zn(OH)_2$ and AgOH hydrophilic colloid leads to greater ADD adsorption capacity on argentite surface and stronger surface hydrophobicity than sphalerite. Flotation tests demonstrate that ADD enables efficient separation of argentite from sphalerite in the pulp containing silver and zinc ions.

Keywords: argentite; sphalerite; ammonium dibutyl dithiophosphate; silver ions; adsorption

1 Introduction

Lead and zinc are widely used in chemical metallurgy, alloy materials and military construction, etc. They have strong sulfur affinity and mostly exist in the form of sulfides, such as galena and sphalerite [1]. Meanwhile, lead and zinc elements are often associated with silver element in geological mineralization processes [2]. Silver element is sulfurophilic and ferrophilic, which makes silver widely distribute in non-ferrous metal deposits. Now numerous associated silver−lead−zinc deposits and independent silver deposits with complex genetic types have been formed [3]. There are nearly 200 species silver-bearing minerals on the earth, but only 12 kinds of silver resources can be developed and have recovery value, among which the main silver ore is argentite [4]. The full optimization of associated silver ore utilization is essential in order to effectively meet the demands of sustained economic growth in China.

At present, most of silver resources in China exist in small associated or symbiotic silver mines with fine particle size and low grade, which makes it difficult to comprehensively utilize [5]. In order to better recover silver-bearing minerals, researchers have carried out a lot of related work. For example,

Corresponding author: *Guan-fei ZHAO, Tel: +86-15573808288, E-mail: fly.guan@163.com;
**Guo-dong LI, Tel: +86-18993398446, E-mail: lgdabcd@163.com

https://doi.org/10.1016/S1003-6326(25)66963-9

Received 25 April 2024; accepted 19 December 2024

JIANG and LI [6] found that the independent silver ores including argentite, freibergite and polybasite existed in the silver-bearing lead−zinc mine in Inner Mongolia (China). With a sulfide ore containing 479.5 g/t silver, which mainly exists in the form of argentite, WANG et al [7] obtained silver grade of 4787.31 g/t and silver recovery of 87.97% through flotation experiments. CHEN et al [8] used ultrasonic pretreatment technology to recover silver from zinc oxide leaching residue, and it was found that ultrasonic pretreatment can obviously improve recovery of silver-containing minerals. JIANG [9] found that the combined lead middle ore regrinding with inhibiting pyrite under low alkali conditions could further improve the silver recovery in lead concentrate. Therefore, it is of great significance to strengthen the recovery of co-associated silver ore resources with the feasible beneficiation technology.

The application and mechanism analysis of reagents in flotation recovery of silver resources are mainly conducted for associated silver ores [10−13]. For example, WANG et al [14] used a chelating collector containing nitrogen functional groups to separate the silver-bearing galena and sphalerite, and the recovery of galena could reach 82% when chelating collector was used. ZHANG et al [15] believed that the —CSS atoms in carrageenan xanthate can be adsorbed to sphalerite surface through active zinc atoms, and realized the separation of silver-bearing galena and sphalerite. QIN [16] found that EMBI, PMBI and BMBI were chemically adsorbed on the associated silver minerals surface through —SH and —NH. Micro-flotation experiments showed that the combination of $KMnO_4$ and CCS could effectively separate silver-bearing galena and sphalerite [17]. FENG et al [18] believed that PBTCA formed C—O—Zn or P—O—Zn bond through carboxyl group and phosphonic acid group complex with Zn site on sphalerite surface, which strongly inhibited sphalerite and had almost no effect on galena, thus achieving flotation separation of silver-bearing galena and sphalerite. Nowadays, the analysis was mainly focused on the galena and sphalerite in silver-bearing lead−zinc ores, and the mechanism of chemical action of independent silver minerals such as argentite, light red silver and stephanite was less systematically studied. Therefore, it was imperative to study the matching and adaptation behavior of independent silver minerals and flotation reagents directly.

The selective collector used in this study was ADD ($(C_4H_9O)_2PSSNH_4$). To investigate the enrichment difference of argentite and sphalerite by ADD, potential depressants such as $ZnSO_4$ and Ag^+ were employed in both pure mineral flotation tests and actual ore flotation tests. Furthermore, a comprehensive analysis combining DFT simulation, zeta potential measurements, adsorption studies, contact angle measurements, and XPS tests was conducted to elucidate the potential adsorption mechanism of ADD. The flotation separation of sphalerite and argentite is an innovative technique, providing a valuable reference for the recovery of silver metal from silver-bearing lead−zinc sulfide ores. This method not only facilitates the efficient separation of silver and zinc but also enhances the enrichment of silver in lead concentrate.

2 Experimental

2.1 Materials and reagents

The pure mineral samples of argentite and sphalerite used in the experiment were produced in Henan Province and Hunan Province in China, respectively. After undergoing a series of procedures including crushing (Rotary crusher), dry grinding (Zirconia ball mill), and screening (Taylor standard sieve), flotation testing was conducted on the mineral particles with size of 0.037−0.074 mm. The X-ray diffraction (XRD) patterns of Fig. 1(a) revealed that the characteristic peaks corresponded to argentite. The XRD pattern depicted in Fig. 1(b) exclusively exhibited distinctive peaks associated with sphalerite, while no characteristic peaks of other substances were observed. As shown in Table 1, the Ag mass fraction was 78.88%, with a argentite purity was 90.56%; the Zn mass fraction was 64.97%, with a sphalerite purity of 96.83%.

The actual ores of polymetallic silver-bearing lead−zinc sulfide was taken from Hunan Province, China. The results of multi-element analysis of the actual ores and the contents of silver-bearing minerals are shown in Table 2 and Table 3. It can be seen from Table 3 that the main silver-bearing mineral was argentite in the actual ores.

Analytical-grade $AgNO_3$ was used as the Ag^+ sources. Ammonium dibutyl dithiophosphate was used as the collector, the analytical grade zinc sulfate

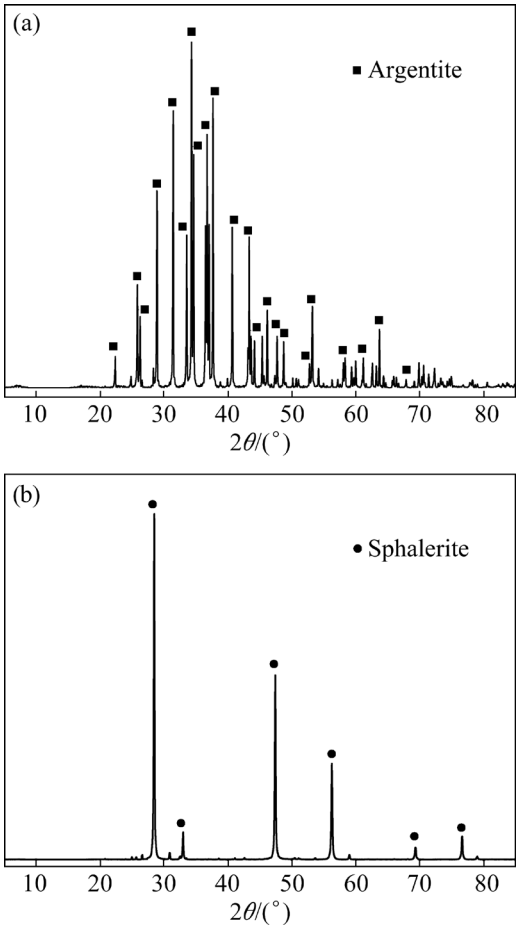

Fig. 1 X-ray diffraction patterns of (a) argentite and (b) sphalerite samples

Table 1 Analysis of main chemical constituents of argentite and sphalerite samples

Sample	Elemental content/wt.%			Purity/wt.%
	Ag	Zn	S	
Argentite	78.88		12.87	90.56
Sphalerite		64.97	31.91	96.83

Table 2 Results of multi-element analysis of actual ores (wt.%)

Pb	Zn	S	SiO_2	MgO	Al_2O_3	As	Ag*
0.84	1.71	4.49	5.61	1.32	6.91	0.28	69.11

*Unit: g/t

Table 3 Contents of silver-bearing minerals (wt.%)

Argentite	Polybasite	Silver−tennatite
85.15	2.62	4.39
Electrum	**Silver-bearing galena**	**Others**
1.18	5.77	0.89

was utilized as the sphalerite depressant, and MIBC served as the flotation frother. The pH of the artificially mixed pulp was adjusted using analytical NaOH and HCl. Ultrapure water was employed in all experiments.

2.2 Molecular simulation (MS) calculation method

The crystal structure of the mineral used in the experiment was obtained from The Materials Project database and optimized for selected crystal cells. Surface models were created by cutting sphalerite (110) and argentite (100). 3×3×2 supercell model was established using these cut crystals, with a vacuum layer of 20 Å to prevent mutual influence of spatially repeated crystal structures. Both adsorption simulation and geometric optimization were conducted using Materials Studio software, while density functional theory (DFT) calculations were performed with the CASTEP module. Non-spin polarization was considered during structure optimization, with GGA-PBE as the electron exchange correlation function and Brillouin region sampled by k point of 3×3×2 grid. The plane wave base set energy cutoff value was chosen as 550 eV, tolerance set to be 1×10^{-5} eV/atom, maximum displacement at 5×10^{-3} Å, max force at 0.03 eV/Å, and max stress at 0.05 GPa. The adsorption binding energy (E_a) is calculated as follows:

$$E_a=E_{s+c}-E_s-E_c \quad (1)$$

where the total energy of the collector and the mineral is represented by E_{s+c}, E_s represents the energy of the exposed surface of the mineral, and E_c represents the energy of the collector. The adsorption energy (E_a) directly characterizes the stability of interaction between reagents and mineral surfaces. The more negative the adsorption energy value, the greater the binding stability of the reagent to the mineral, thereby enhancing its selectivity towards the mineral.

2.3 Inductively coupled plasma (ICP) analysis

The concentration of metal ions in mineral flotation pulp solution was determined by Optima 8300DV ICP spectrometer. 2 g mineral sample was mixed with deionized water using a magnetic stirrer. Subsequently, the supernatant was recovered to determine the concentration of silver ions. Then, appropriate amount of supernatant was mixed with sphalerite powder to re-evaluate the silver ion

concentration. This process was repeated three times and the average was determined.

2.4 Zeta potential measurement

Malvern Zetasizer Nano ZS90 potentiometric analyzer was utilized for the measurement. Each sample was subjected to ultrafine grinding prior to preparation. Subsequently, 15 μm powder sample was placed within a beaker containing 40 mL of 0.01 mol/L KCl reagent as the background solution, followed by blending for 10 min using a magnetic mixer. Thereafter, 5 mL aliquot of the suspension was withdrawn for zeta potential determination. This measurement was replicated three times to calculate the average.

2.5 X-ray photoelectron spectroscopy measurement

Refined XPS analysis was conducted using the Thermo Scientific K_α system, utilizing Model 250X. The diffraction analysis was executed within an energy range of 20 eV. The mineral samples prepared for testing adhered to the protocols established for the single mineral flotation experiment. Following sample preparation, four washes with ultrapure water were performed, and subsequently, the samples were filtered and vacuum-dried at a low temperature (35−45 °C). Prior to XPS examination, the solid samples were pulverized and homogenized to ensure the uniformity.

2.6 Adsorption measurement

The adsorption capacity was quantitatively assessed via ultraviolet spectrophotometry, utilizing full spectrum scanning with the Elementar TOCII instrument (manufactured by Elementar Co., Langenselbold, Germany) for the ADD reagent. In the sample preparation process, a copper ion chromogenic agent and an extraction method were employed. Subsequently, the organic phase was transferred to a quartz cuvette for the determination of the UV spectrum. The distinct absorption peak of ammonium dibutyl dithiophosphate (ADD) in the ultraviolet spectrum is located at 435 nm. Triplicate measurements were conducted for each test, and the results were subjected to statistical averaging.

2.7 Contact angle measurement

The mineral bulk with the smallest crack and plane was selected for the contact angle measurement. The samples were thoroughly polished using 13 μm polishing disc on Tegramin−25 polishing machine and then air-dried. The sample was analyzed using the JY−82C analyzer to detect and compare the contact angles generated by the ultra-pure water droplets and various reagents on the surface of the mineral sample. The experiment was repeated three times, expressed as average values.

2.8 Flotation experiments

The flotation test was conducted using the XFDIV 3.0 hanging flotation machine. The massive ore underwent crushing and homogenization processes. The 1000 g portion of silver-bearing polymetallic lead−zinc sulfide was extracted from the homogenized ore sample and placed into a ball mill for fine grinding. Subsequently, the finely ground sample was transferred to 3 L flotation cell where pH regulator, depressant, collector, and frother were sequentially added (as depicted in Fig. 2). The pure mineral flotation test was performed using the XFGII2 type hanging tank flotation machine. In each test, 2 g of argentite and sphalerite were taken and subjected to ultrasonic cleaning in an ultra-pure water-filled beaker for 3 min to remove any oxide layer on the mineral surface. The cleaned mineral sample was then placed into 40 mL micro-flotation cell with the spindle speed of the flotation machine adjusted to 1840 r/min. Both foam concentrate products and tank products were filtered at room temperature under vacuum conditions before being dried and weighed accordingly. The formula used to calculate mineral recovery (ε) in the flotation test is as follows:

$$\varepsilon=m_1/(m_1+m_2)\times100\% \quad (2)$$

where m_1 and m_2 represent masses of foam concentrate product and tailings product, respectively.

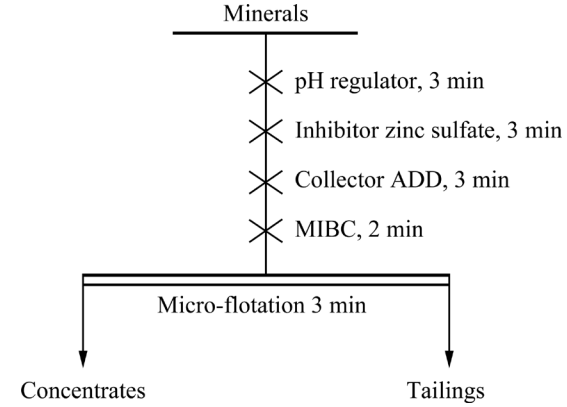

Fig. 2 Flowsheet of microflotation experiment

3 Results and discussion

3.1 MS calculation of ADD adsorption on argentite and sphalerite

According to the principles of DFT theory, the CASTEP module can be utilized to analyze the adsorption model and energy of flotation reagent molecules on mineral surfaces. MS was used to elucidate the adsorption mechanism of four methylamine cations on three Fe(II/III)−kaolinite surfaces and the microscopic effects of Mg(II) doping amount on the hydration characteristics of kaolinite surface were explored [19,20]. LIAO et al [21] employed DFT calculations to demonstrate the chemisorption interaction between SBX molecules and chlorite as well as pyrite. The differences in the sulfidization mechanism of cerussite and smithsonite were comparatively studied by DFT method [22]. The selective adsorption difference of ADD on argentite and sphalerite was analyzed through X-ray diffraction measurement and DFT adsorption energy calculation [23]. The optimized structures of ADD, argentite, and sphalerite are depicted in Fig. 3. The adsorption of ADD on the (100) surface of argentite and the (110) surface of sphalerite is illustrated in Fig. 4. Table 4 presents the adsorption energy values for argentite and sphalerite following their interaction with ADD.

The energies of argentite and sphalerite are −112001.0465 and −63660.2806 eV, respectively, and the energy of ADD is −3139.8336 eV. It could be seen from Fig. 4 and Table 4 that ADD interacts with argentite and sphalerite to form S—P bonds, and the bond lengths with argentite and sphalerite are 2.490−2.510 Å and 2.328−2.329 Å, respectively. The bond lengths of adsorption bonds are shorter than the sum of their respective ionic radii, indicating that ADD molecules exist on argentite and sphalerite through chemisorption. When the adsorption of ADD on the surfaces of argentite and sphalerite reaches equilibrium, the adsorption energies on argentite and sphalerite surface are −1.794 and −0.422 eV, respectively. The more negative adsorption energy of ADD on argentite surface compared to that on sphalerite indicates higher adsorption stability for ADD on argentite.

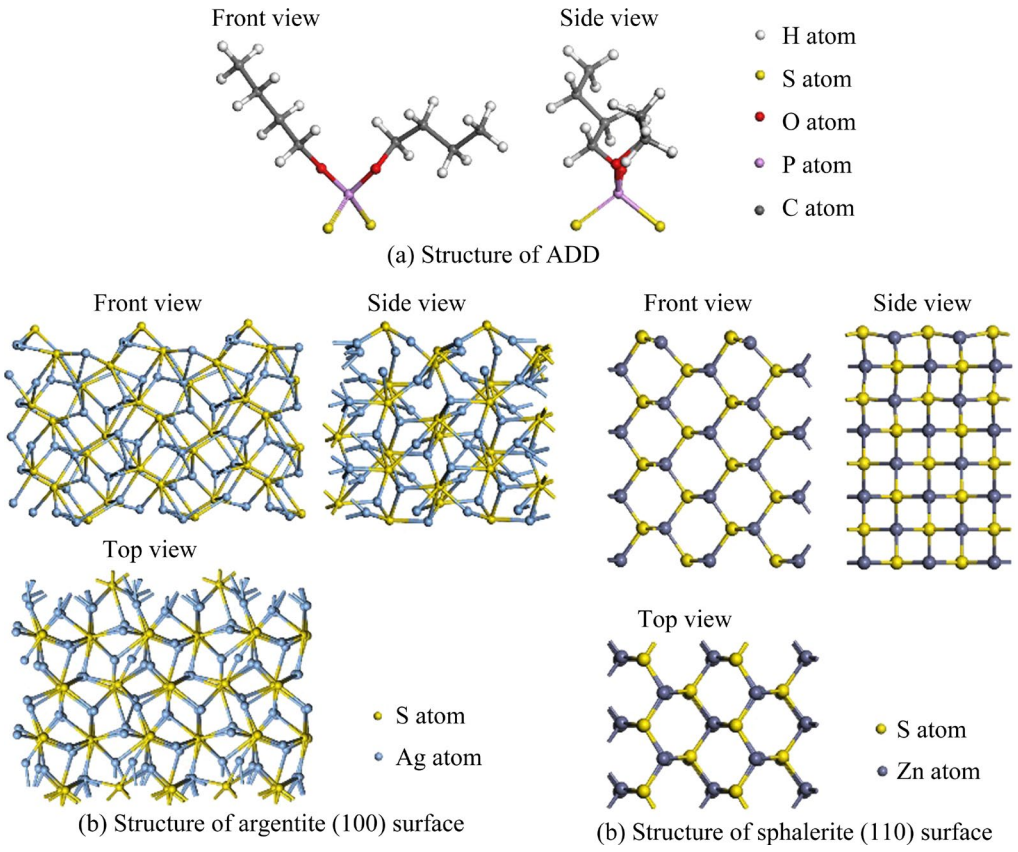

Fig. 3 Crystal structure of (a) ADD, (b) argentite and (c) sphalerite

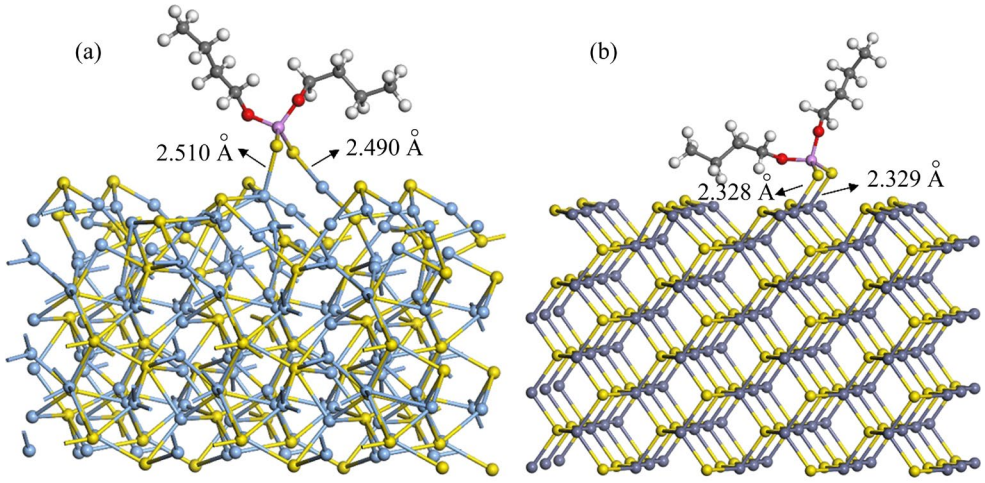

Fig. 4 ADD adsorbted on (a) argentite (100) surface, and (b) sphalerite (110) surface

Table 4 Adsorption energy and bond length of argentite and sphalerite after interaction with ADD

Sample	Total energy/eV	Adsorption energy/eV	Bond length/Å
Argentite	−115142.6743	−1.7941	2.490−2.510
Sphalerite	−66800.5363	−0.4220	2.328−2.329

3.2 Ag^+ contents in varied pulp and ionic hydrolyzed component analysis

It is demonstrated that the presence of metal ions in pulp exerts an influence on the floatability of sphalerite through the mechanisms of substitution, adsorption, and coating [24]. The mixed pulp solution of argentite and sphalerite contains primarily silver ions and zinc ions. Silver ions can activate the surface of sphalerite through lattice substitution and surface adsorption, which significantly impacts the adsorption behavior of collector molecules on the sphalerite surface [25]. Hence, it is imperative to conduct an analysis on the variation of silver ions within the pulp. Throughout the experiment, a synthetic mixture of argentite and sphalerite (consisting of 1.5 g argentite and 0.5 g sphalerite) was utilized in a ratio of 3:1. In the ADD concentration system of 6×10^{-6} mol/L, an investigation was conducted on the composition and state of various silver ions in a mixed pulp, with magnetic stirring performed within a time range of 10−30 min. The distribution of Ag^+ content in different pulps is illustrated in Fig. 5. In the alkaline pulp solution, the main silver ionic hydrolyzed components are divided into AgOH, Ag_2O and $Ag(OH)_2^-$, and the reaction equation is as follows:

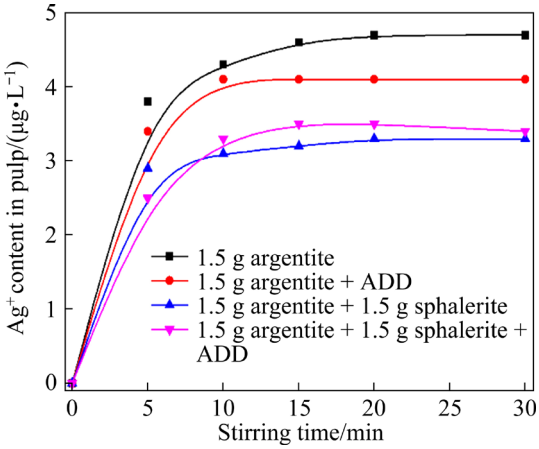

Fig. 5 Ag^+ contents at different stirring time for various mixed pulp

$$Ag^+ + OH^- \rightarrow AgOH \quad (3)$$

$$2AgOH \rightarrow Ag_2O + H_2O \quad (4)$$

$$AgOH + OH^- \rightarrow Ag(OH)_2^- \quad (5)$$

The stirring time, as depicted in Fig. 5, not only signifies the duration of interaction between minerals and reagents but also characterizes the propensity for Ag^+ dissolution from the surface of argentite. (1) The Ag^+ content within the slurry solution exhibits a significant increase during the initial 15 min, accompanied by an extended stirring time. However, once surpassing a stirring time of 20 min, the Ag^+ content within the pulp system tends to stabilize. (2) When 0.5 g of sphalerite is introduced to argentite, the concentration of Ag^+ in the pulp significantly decreases from 4.7 to 3.3 μg/L, indicating that the missing Ag^+ ions are adsorbed onto the surface of sphalerite. (3) The concentration

of silver ions decreases from 4.7 to 4.2 μg/L after the addition of ADD to the pulp, indicating that the adsorption of ADD on the surface of the argentite can mitigate the dissolution of Ag^+ on its surface. (4) When ADD is added to the argentite and sphalerite mixed pulp, the Ag^+ contents increase slightly from 3.3 to 3.5 μg/L after the stirring time over 10 min, indicating that ADD and Ag^+ have competitive adsorption, and ADD hinders the adsorption of Ag^+ on the surface of sphalerite.

3.3 Zeta potential

The modification of local ion concentration in the solution and the adsorption of reagent molecules onto the surface of mineral particles can alter the potential difference between the mineral surface and the solution [26,27]. The coexistence of argentite and sphalerite pulp makes it easier for dissolved silver ions to adsorb to the surface of sphalerite, with the concentration of ADD of 6×10^{-6} mol/L, and the concentration of Ag^+ of 4×10^{-3} mg/L.

The zeta potentials of argentite and sphalerite in Ag^+ and ADD systems at various pH values are illustrated in Fig. 6. The determination of zeta potential in ultra-pure water reveals that the presence of Ag^+ ions induces a negative shift in the zeta potential of argentite across different pH ranges, while the zeta potential of sphalerite experiences a positive shift. This observation suggests that Ag^+ particles can be adsorbed onto the surface of sphalerite. Compared with the zeta potential of argentite and sphalerite in the Ag^+ systems at different pH levels, a negative shift of argentite and sphalerite occurs upon the addition of ADD, which indicates that ADD can be adsorbed on the argentite and sphalerite surfaces, and when the pulp pH was 8,

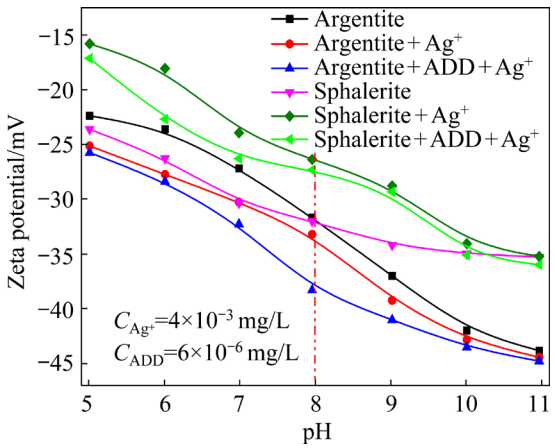

Fig. 6 Zeta potential of argentite and sphalerite

the surface potential of argentite decreases from −33.19 to −38.28 mv (a decrease of −5.09 mV), while the surface potential of sphalerite decreases from −26.35 to −27.30 mV (a decrease of −0.95 mV). Hence, it can be inferred that the presence of Ag^+ on the surface of sphalerite may lead to its adsorption, thereby impeding the adsorption of ADD. Consequently, the adsorption capacity of ADD on argentite surfaces is significantly higher compared to that on sphalerite surfaces.

3.4 XPS analysis of Ag^+ and ADD on sphalerite surface

The measurement of adsorption capacity can directly reflect the affinity between metal ions and reagent molecules with the mineral particle surface. LAN et al [28] used XPS detection to analyze the adsorption of gallic acid on the surface of apatite and dolomite. LIU et al [29] found that hydrogen peroxide can promote the surface of galena to produce more hydrophilic hydroxide through XPS detection. In this work, XPS analysis was utilized to further examine the alterations in chemical states of surface elements with sphalerite and argentite by ADD adsorption, with the Ag^+ concentration of 4×10^{-3} mg/L, and the ADD concentration of 6×10^{-6} mol/L.

The scanning XPS spectra of argentite and sphalerite before and after the action of ADD reagent are presented in Fig. 7. As depicted in Fig. 7(a), after the reaction of argentite with ADD, it is evident that a characteristic P 2p peak emerges, representing the phosphorus element of ADD molecule. This observation signifies the robust adsorption capability of ADD on argentite surface. Characteristic peaks of Zn 2p, S 2p, and C 1s appear, as depicted in Fig. 7(b). Following the reaction between sphalerite and Ag^+, the spectrum reveals the Ag 3d characteristic peak, indicating that Ag^+ is adsorbed onto sphalerite surface. After the reaction of sphalerite with Ag^+ and ADD, the emergence of a characteristic P 2p peak happens, while the Ag 3d characteristic peak diminishes, indicating competitive adsorption between ADD and Ag^+, and ADD hinders the adsorption of Ag^+ on sphalerite surface. This is consistent with the analyses of Ag^+ contents at different stirring time for various mixed pulp. Meanwhile, the extended Ag 3d and P 2p scanning spectra are shown in Fig. 8.

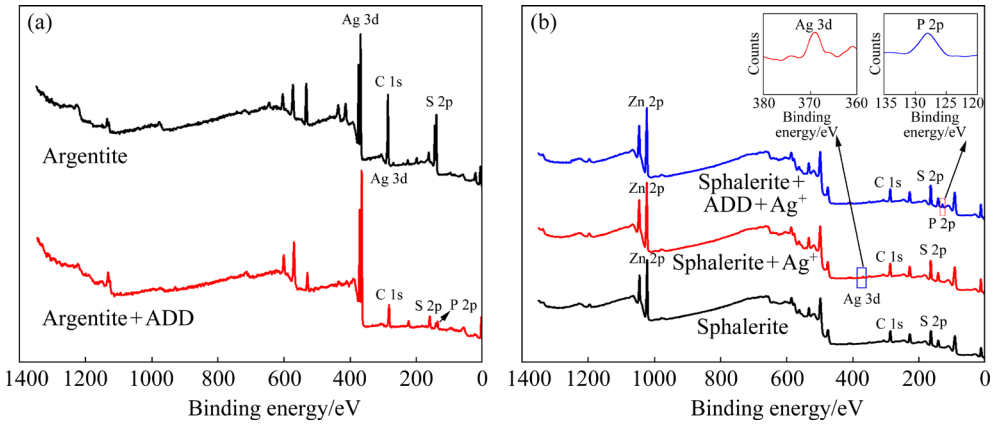

Fig. 7 XPS survey scan spectra of (a) argentite and (b) sphalerite samples before and after adding ADD

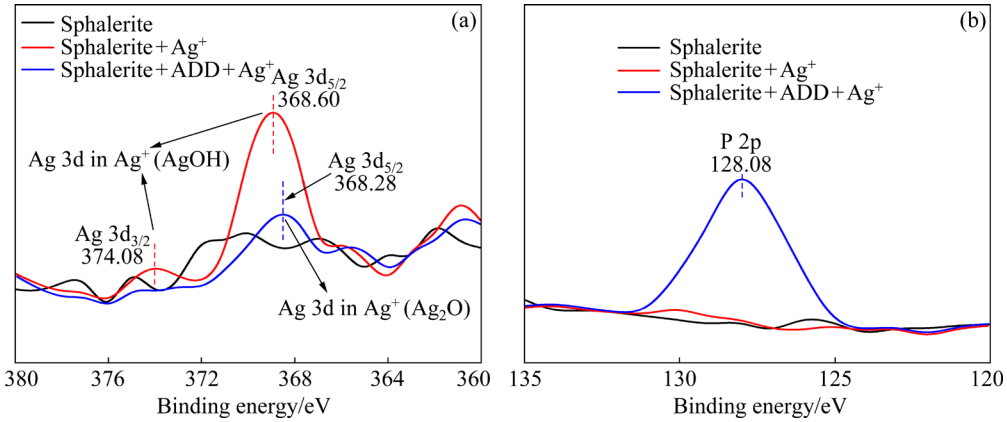

Fig. 8 (a) Ag 3d and (b) P 2p XPS scan spectra of sphalerite sample before and after adding Ag^+ and ADD

The changes in the relative content of corresponding elements on argentite and sphalerite surface before and after ADD reaction are illustrated in Table 5 and Table 6, respectively. Following the ADD reaction, there is a significant increase of 15.89% in the relative content of P 2p on argentite, whereas only a marginal increase of 1.37% is observed on sphalerite, indicating that the amount of ADD adsorbed on argentite surface is obviously greater than that on sphalerite surface, and the hydroxide of silver prevents the adsorption of ADD on sphalerite surface. Meanwhile, after adding ADD, the content of Ag 3d on sphalerite surface decreases by 0.06%, indicating that there is competitive adsorption between ADD and Ag^+.

Table 5 Argentite binding energy and Ag 3d/P 2p contents before and after adding ADD

Sample	Binding energy/eV		Content/%	
	Ag 3d	P 2p	Ag 3d	P 2p
Argentite	367.38	–	18.89	–
Argentite + ADD	367.41	137.57	20.16	15.89

Table 6 Sphalerite binding energy and Ag 3d/P 2p contents before and after adding Ag^+ and ADD

Sample	Binding energy/eV		Content/%	
	Ag 3d	P 2p	Ag 3d	P 2p
Sphalerite	–	–	–	–
Sphalerite + Ag^+	369.08	–	0.11	–
Sphalerite + ADD + Ag^+	369.88	128.08	0.05	1.37

3.5 Adsorption capacity of ADD and wettability on argentite and sphalerite surface

The variation in adsorption capacity among mineral surface flotation reagents indicates the selectivity of these reagents towards different minerals, and this selectivity ultimately manifests in the recovery of diverse minerals through flotation. TAN et al [30] found that sodium diethyl dithiocarbamate was strongly adsorbed on the surface of galena, and the separation of galena and sphalerite can be realized by adding zinc sulfate after the addition of sodium diethyl dithiocarbamate. CHENG et al [31] believed that the hydrophobic

products of ADD adsorbed on galena surface were mainly elemental sulfur and collector metal salt. In this adsorption capacity measurement, pulp concentration was 10 g/L, Ag^+ concentration was 4×10^{-3} mg/L, $ZnSO_4$ concentration was 6×10^{-5} mol/L, and ADD concentration was 6×10^{-6} mol/L.

The adsorption effect of ADD on the argentite and sphalerite surface is illustrated in Fig. 9 with the coexistence of Ag^+ and $ZnSO_4$. As depicted in Fig. 9, with the pH value increasing from 5 to 8, the adsorption capacity of ADD on argentite surface rises from 0.33 to 0.82 mg/g. Subsequently, with a further increase in pH to 11, the adsorption capacity of ADD decreases to 0.48 mg/g. When Ag^+ and $ZnSO_4$ are added to the pulp, ADD adsorption capacity on argentite surface decreases slightly, and the maximum adsorption capacity decreases from 0.82 to 0.80 mg/g. The adsorption of ADD on sphalerite surface increases from 0.32 to 0.73 mg/g as the pH rises from 5 to 8. However, with further increase in pH to 11, the adsorption capacity of ADD decreases to 0.45 mg/g. When Ag^+ and $ZnSO_4$ are added to pulp, ADD adsorption capacity on sphalerite surface decreases significantly, and the maximum adsorption value decreases from 0.73 to 0.27 mg/g. The above analyses show that when Ag^+ and $ZnSO_4$ are added to the pulp, the adsorption capacity of ADD on argentite surface has little change, but the adsorption capacity of ADD on sphalerite surface significantly decreases.

The contact angle is inversely proportional to the hydrophilicity of the mineral surface [27]. It is mentioned that testing of contact angle requires the solid to possess an ideally smooth surface, and variations in surface roughness and uniformity can impact the test results [32,33]. In this contact angle measurement, the pH of pulp was 8.0, Ag^+ concentration was 4×10^{-3} mg/L, $ZnSO_4$ concentration was 6×10^{-5} mol/L, and ADD concentration was 6×10^{-6} mol/L.

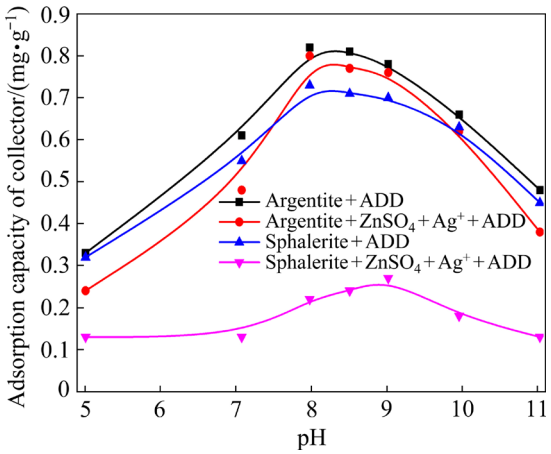

Fig. 9 ADD adsorption on argentite and sphalerite surface with coexistence of Ag^+ and $ZnSO_4$

The contact angles of argentite and sphalerite in ultrapure water, Ag^+ + ADD and $ZnSO_4$ + Ag^+ + ADD systems are presented in Fig. 10. The contact angles of argentite and sphalerite in ultrapure water are measured as 66.7° and 64.7°, respectively, indicating a comparable natural hydrophilicity between molybdenite and sphalerite. After adding Ag^+ + ADD, the contact angle of argentite and sphalerite are increased to 89.2° and 65.1°, respectively. It is indicated that the adsorption capacity of ADD on the argentite surface is higher than that of sphalerite, maybe due to the competitive adsorption of AgOH hydrophilic colloid and ADD on sphalerite surface, and AgOH hydrophilic colloid preventing

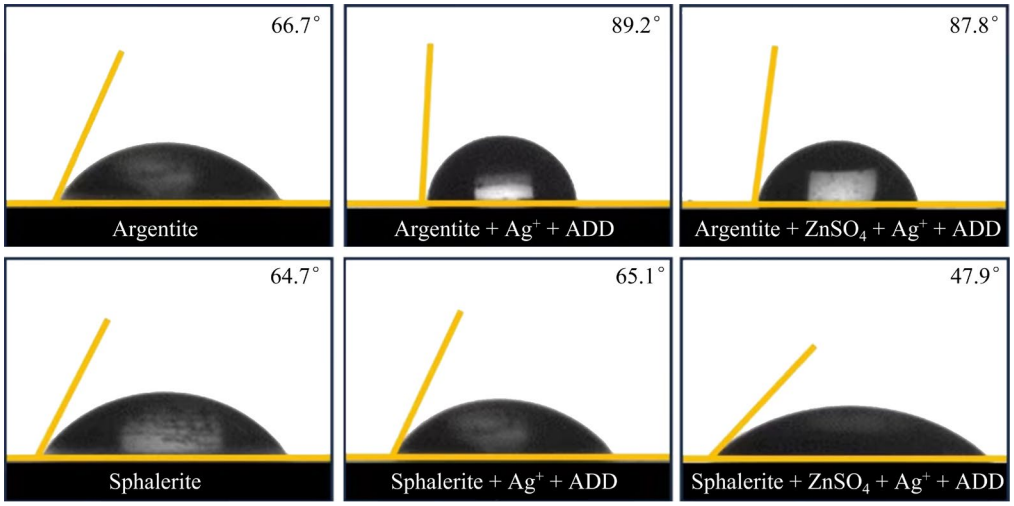

Fig. 10 Contact angle of argentite and sphalerite after interaction with ADD, Ag^+ and $ZnSO_4$

the adsorption of ADD on sphalerite surface. After adding $ZnSO_4$ + Ag^+ + ADD, the contact angle of argentite and sphalerite are increased to 87.8° and 47.9°, respectively. It is indicated the adsorption of $Zn(OH)_2$ and AgOH hydrophilic colloid on sphalerite surface is strong, which prevents the adsorption of ADD on sphalerite surface. But the adsorption of $Zn(OH)_2$ and AgOH hydrophilic colloid on argentite surface is weak, and hence more ADD molecules are adsorbed on argentite surface.

3.6 Flotation results

3.6.1 Effects of pulp pH on argentite and sphalerite recovery

Pulp pH is a very important parameter in the flotation separation of argentite and sphalerite. The pH of the slurry can affect the existing forms of metal ions and the surface electrical properties of minerals [34]. The floatability of argentite is found to be superior in a weak alkaline environment with a pH range of 9−10, while it exhibits a significant reduction in floatability when exposed to strong alkaline conditions with a pH exceeding 11 [35]. The findings of various studies have demonstrated that the pH value has the capability to alter the electrochemical environment within the pulp, thereby exerting an influence on the floatability of galena and sphalerite [36]. In order to realize the secondary recovery of lead and zinc resources in sulfur concentrate, DENG et al [37] used lime to adjust the pH value of pulp and obtained a sulfur concentrate with the sum of lead and zinc grade of 0.98%. The flotation recovery rates of argentite and sphalerite are depicted in Fig. 11, with the addition concentration set at 6×10^{-6} mol/L ADD and 1×10^{-6} mol/L MIBC.

The analysis of Fig. 11 reveals the following findings: argentite and sphalerite demonstrate distinct flotation recovery trends in response to varying pH conditions. As the pH value increases from 2.0 to 8.0, the recovery rate of argentite gradually rises, reaching a maximum of 82.36%. However, when the alkaline slurry system reaches a pH of 12, the recovery rate of argentite slowly declines to 48.38%. This indicates that both highly acidic and highly alkaline conditions are unfavorable for argentite flotation. Conversely, the recovery rate of sphalerite exhibits a continuous increase as the pH level is elevated from 2 to 12, with a gradual ascent observed within pH range of 8−12. Consequently, it can be determined that the optimal pH value for subsequent separation of argentite and sphalerite is 8.0.

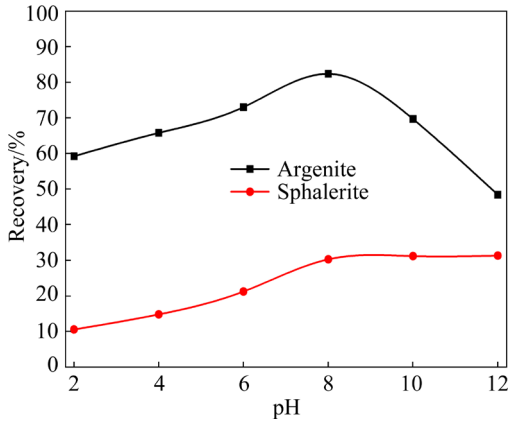

Fig. 11 Effect of pulp pH on recovery of argentite and sphalerite

3.6.2 Effects of adding $ZnSO_4$ + Ag^+ and ADD on argentite and sphalerite recovery

The hydrolysis of $ZnSO_4$ in an alkaline solution results in the formation of zinc hydroxide [$Zn(OH)_2$]. These hydrophilic colloidal species are subsequently adsorbed onto the surface of sphalerite, making it a highly effective inhibitor for sphalerite [38]. Ag^+ can be chemically adsorbed on sphalerite surface by Ag—S bond [39]. In this work, the flotation recoveries of argentite and sphalerite are presented in Fig. 12, where the pulp pH value was 8.0, MIBC concentration was 1×10^{-6} mol/L, Ag^+ concentration was 4×10^{-3} mg/L, $ZnSO_4$ concentration was 6×10^{-5} mol/L, and the varied ADD concentration was set in the test.

The results presented in Fig. 12 can be inferred as follows: (1) The maximum recovery of argentite reaches 84.36% when the ADD concentration is 6×10^{-6} mol/L. (2) After the addition of Ag^+ + ADD, there is minimal alteration in the recovery of argentite, whereas a noticeable decrease is observed in the recovery of sphalerite. This phenomenon can be attributed to the hydrophilic colloid AgOH hindering the adsorption of ADD on the surface of sphalerite. (3) After adding $ZnSO_4$ + Ag^+ + ADD, the recovery of argentite has a slight decline, while the recovery of sphalerite has decreased significantly. The results demonstrate that the adsorption capacity of ADD on the argentite surface remains nearly unchanged, whereas a significant decrease in the adsorption capacity of ADD on the sphalerite surface is observed. This could potentially be attributed to

the hydrophilic colloids AgOH and $Zn(OH)_2$ hindering the adsorption of ADD onto the sphalerite surface.

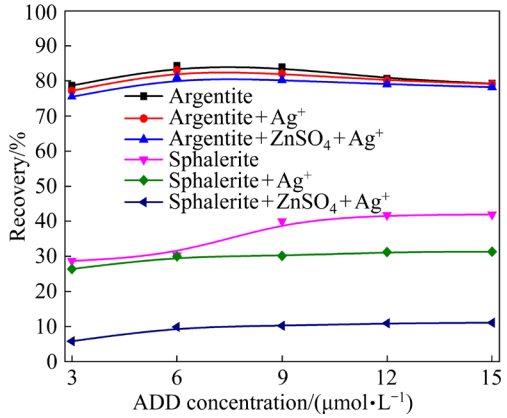

Fig. 12 Effect of ADD with Ag^+ and $ZnSO_4$ on argentite and sphalerite recovery

3.6.3 Effects of ADD adsorption on Ag recovery of mixed minerals and actual ores

The artificial mixed ore flotation test was conducted to further validate the differential selective adsorption of argentite and sphalerite by ADD before and after the addition of $ZnSO_4 + Ag^+$. As depicted in Table 7, when only ADD is introduced, the concentrate product exhibits an Ag grade of 53.76% with a recovery rate of 72.65%. When ADD + $ZnSO_4$ + Ag^+ are combined, there is a slight increase in the recovery of silver, reaching 75.78%. Additionally, there is a significant enhancement in the silver grade, which rises to 64.17%. Therefore, the artificial mixed flotation results demonstrate that the adsorption capacity of ADD on the surface of argentite significantly surpasses that of sphalerite. Moreover, ADD exhibits superior performance in facilitating the flotation separation between argentite and sphalerite in $ZnSO_4 + Ag^+$ system.

In order to verify the flotation separation effect of ADD on argentite and sphalerite in the $ZnSO_4 + Ag^+$ system, collector ADD and ethyl xanthate (EX) were chosen for conducting actual polymetallic silver-bearing lead−zinc sulfide flotation experiment. The experimental results are presented in Table 8. It is evident that the flotation separation efficiency of ADD on argentite and sphalerite in the $ZnSO_4 + Ag^+$ system surpasses that of EX, enabling the recovery of lead concentrate with an impressive Ag grade of 1982.91 g/t and a remarkable Ag recovery rate of 70.87%. The actual flotation results of the ores have demonstrated that ADD can achieve a favorable recovery of silver in polymetallic silver-bearing lead−zinc sulfide.

Table 7 Flotation results of mixed minerals

Condition	Product	Yield/%	Ag grade/%	Ag recovery/%
Adding ADD	Concentrate	52.85	53.76	72.65
	Tailing	47.15	22.69	27.35
	Feed	100.00	39.11	100.00
Adding ADD + $ZnSO_4$ + Ag^+	Concentrate	46.22	64.17	75.78
	Tailing	53.78	17.63	24.22
	Feed	100.00	39.14	100.00

1 g argentite: 1 g sphalerite; pH=8.0; $C_{Ag^+}=4\times10^{-3}$ mg/L; $C_{ZnSO_4}=5\times10^{-6}$ mol/L; $C_{ADD}=6\times10^{-6}$ mol/L; $C_{MIBC}=1\times10^{-6}$ mol/L)

Table 8 Flotation results of actual ores

Condition	Product	Yield/%	Ag grade/($g\cdot t^{-1}$)	Ag recovery/%
60 g/t ADD	Lead concentrate	2.47	1982.81	70.87
	Zinc concentrate	3.09	120.22	5.38
	Tailing	94.44	17.39	23.75
	Actual ore	100.00	69.11	100.00
60 g/t EX	Lead concentrate	2.69	1801.75	70.13
	Zinc concentrate	3.35	133.13	6.45
	Tailing	93.96	17.22	23.42
	Actual ore	100.00	69.11	100.00

500 g actual ores; pH=8.5; w_{Ag^+}=12 g/t; w_{ZnSO_4}=400 g/t; w_{ADD}=60 g/t; w_{EX}=60 g/t

In order to visually illustrate the adsorption morphology and trends of argentite and sphalerite surfaces before and after addition of $ZnSO_4 + Ag^+$, a model depicting the interaction between various reagents and mineral micro-surfaces is constructed, as shown in Fig. 13. After the addition of ADD + Ag^+ + $ZnSO_4$, a large amount of $Zn(OH)_2$ and AgOH hydrophilic colloid particles are adsorbed onto the sphalerite surface, while almost no hydrophilic colloidal particles are adsorbed onto the argentite surface. These $Zn(OH)_2$ and AgOH hydrophilic colloid particles hinder the adsorption of ADD on the sphalerite surface, resulting in a significantly higher adsorption capacity of ADD on the argentite surface. This observation suggests that in Ag^+ and $ZnSO_4$ system, ADD can effectively achieve flotation separation between argentite and sphalerite.

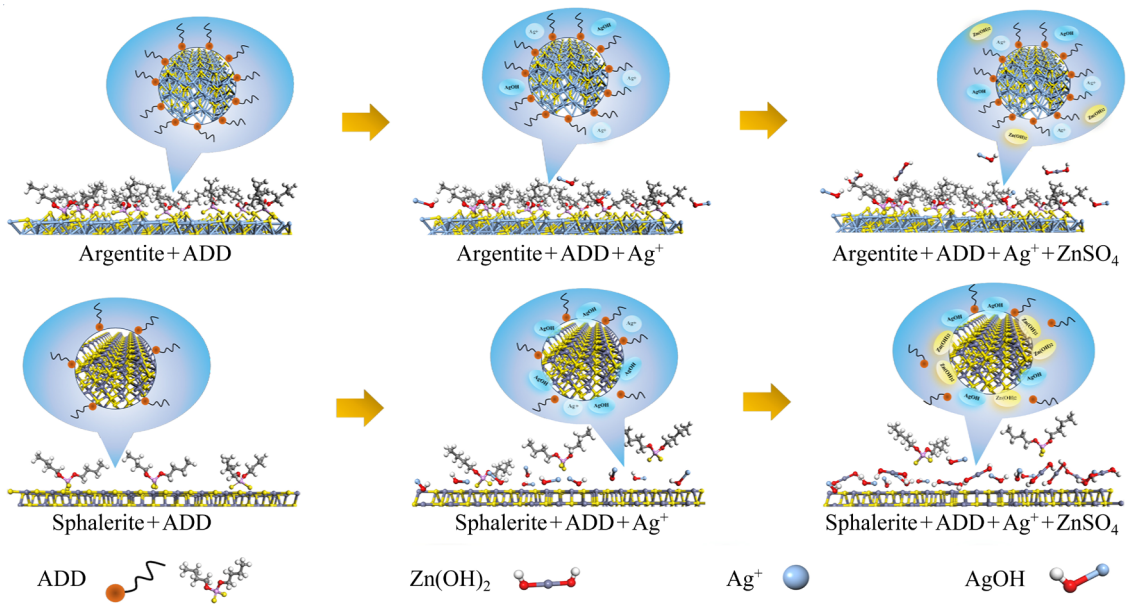

Fig. 13 Schematic illustration of ADD adsorption on argentite and sphalerite surface

4 Conclusions

(1) ADD is chemisorbed on argentite and sphalerite surface by S—P bond, and the adsorption energy between ADD and argentite is stronger than that between ADD and sphalerite.

(2) In ADD + Ag^+ system, the dissolved Ag^+ from argentite surface can be absorbed on sphalerite surface in the form of silver hydroxide, and AgOH hydrophilic colloid can prevent the adsorption of ADD on sphalerite surface; in ADD + $ZnSO_4$ + Ag^+ system, $Zn(OH)_2$ and AgOH hydrophilic colloid can prevent the adsorption of ADD on sphalerite surface, and thereby the adsorption capacity of ADD on argentite surface is much greater than that of sphalerite.

(3) In the flotation experiment of artificial mixed minerals, the concentrate with Ag grade of 64.17% and Ag recovery of 75.78% are obtained. In the flotation experiment of actual ores, lead concentrate with Ag grade of 1982.91 g/t and Ag recovery of 70.87% can be obtained. Therefore, it can be found that ADD can achieve efficient flotation separation of argentite from sphalerite in $ZnSO_4$ + Ag^+ system.

(4) Flotation separation of sphalerite and argentite is an innovative technique, and it can provide a valuable reference for the recovery of silver metal from silver-bearing lead−zinc sulfide ores.

CRediT authorship contribution statement

Ting-sheng QIU: Resources, Methodology, Supervision; **Kai-wei DING:** Testing, Data curation, Data analysis; **Guan-fei ZHAO:** Methodology, Investigation, Validation, Formal analysis, Writing − Original draft; **Guo-dong LI:** Writing − Review & editing, Supervision; **Wen-hui YANG:** Writing – Review & editing; **Hao CHENG:** Writing – Review & editing; **Shun-de YAN:** Testing, Writing – Review & editing.

Declaration of competing interest

The authors declare that they have no known competing financial interests or personal relationships that could have appeared to influence the work reported in this paper.

Acknowledgments

The authors gratefully acknowledge the support from the National Key Research and Development Program of China (No. 2022YFC2904504), the Science and Technology Research Project of Jiangxi Provincial Department of Education, China (No. GJJ2200864), and the Gansu Provincial Key Research and Development Project, China (No. 22YF7GA073).

References

[1] LIU Ying-chao, YANG Zhu-seng, YU Yu-shuai, MA Wang, YUE Long-long, TANG Bo-lang. Characteristics and genesis of the Zhaofayong karst-controlled MVT deposit in the Changdu region, Tibet [J]. Acta Geoscientica Sinica, 2019,

40(6): 853−870. (in Chinese)

[2] ZHOU Xiao-kang, LI Wei-cheng, DONG Wang-cang, ZHOU Bin. A preliminary study of the characteristics of lead-zinc deposits in Shanxi province and their distribution laws [J]. Northwestern Geology, 2020, 53(3): 127−139. (in Chinese)

[3] WANG Geng-chen. Study on flotation separation of silver-bearing lead−zinc sulfide ores [D]. Northeastern University, 2008. (in Chinese)

[4] MA Zhong-yuan, ZHANG Ai-kui, LI Jun, MA Qiang, ZHANG Cai-xia, WANG Lin. Study on the occurrence status of silver polymetallic minerals in the V-belt of Harizha deposit in East Kunlun [J]. Journal of Qinghai University, 2023, 41(6): 78−87. (in Chinese)

[5] ZHAO Zhi-qiang, LIAO Jian-cheng, HE Zheng, LUO Ke-hua, MA Bin, HU Yang-jia. The research and application of new technology to improve the separation index of silver bearing lead-zinc ore in Qixia mountain [J]. Non-ferrous Metals (Beneficiation), 2019(5): 63−70, 80. (in Chinese)

[6] JIANG Lin, LI A-jun. Study on process mineralogy for a silver-containing lead-zinc ore in inner Mongolia [J]. Multipurpose Utilization of Mineral Resources, 2020(1): 94−97. (in Chinese)

[7] WANG Yi-jie, WEN Shu-ming, LIU Dian-wen, LIU Dan. Research on properties and flotation feasibility of a silver ore associated with copper in Yunnan [J]. Advanced Materials Research, 2013, 868: 447−450.

[8] CHEN Can-neng, ZHANG Song, LIU Quan-jun, CHEN Lu-zheng, XIAN Yong-jun. Ultrasonic pretreatment for enhancing flotation separation of elemental sulfur and silver-bearing lead minerals from an oxidative pressure leaching residue of zinc sulfide [J]. Minerals Engineering, 2024, 205: 108495.

[9] JIANG Huang-yi. Experimental study on occurrence and recovery of silver in a lead-zinc mine [J]. Non-ferrous Metals (Beneficiation), 2023(2): 116−123. (in Chinese)

[10] SUN Wei, SU Jian-fang, ZHANG Gang, HU Yue-hua. Separation of sulfide lead-zinc-silver ore under low alkakinity condition [J]. Journal of Central South University, 2012, 19: 2307−2315.

[11] NEET A, GLAY B, ALIM G, OLGA K, FRAT K, OZAN K, GVEN N. The effect of collector's type on gold and silver flotation in a complex ore [J]. Separation Science and Technology, 2011, 46(2): 283−289.

[12] ZHANG Fa-jun, XU Yong-wei, ZHOU Hua-rong, GUO Wan-zhong, BAI Ya-lin, PENG Gui-xiong. Experimental study and production practice on improving the recovery of associated gold and silver in Xitieshan lead-zinc mine [J]. Non-ferrous Metals (Beneficiation), 2023(5): 100−105. (in Chinese)

[13] QIU Ting-sheng, DONG Hao, YAN Hua-shan, WU Hao. Separation of low alkali copper and sulfur and comprehensive recovery of associated gold and silver from a gold, silver, copper and sulfur ore [J]. Non-ferrous Metals Science and Engineering, 2021, 12(5): 81−88. (in Chinese)

[14] WANG Jing-gang, JI Yue-han, CHENG Shao-yi, LIU Shu, CAO Jian, CHEN Pan. Selective flotation separation of galena from sphalerite via chelation collectors with different nitrogen functional groups [J]. Applied Surface Science, 2021, 568: 150956.

[15] ZHANG Yue, ZHANG Xiao-lin, LIU Xin-xin, CHANG Tian-cang, NING Shuai, SHEN Pei-lun, LIU Rui-zeng, LAI Hao, LIU Dian-wen, YANG Xin-yu. Carrageenan xanthate as an environmental-friendly depressant in the flotation of Pb−Zn sulfide and its underlying mechanism [J]. Colloids and Surfaces A: Physicochemical and Engineering Aspects, 2022, 653: 129926.

[16] QIN Wei. Design, synthesis and flotation mechanism study on flotation reagents for silver containing lead-zinc ore [D]. China University of Mining and Technology (Beijing), 2013. (in Chinese)

[17] CHEN Yuan-gan, FENG Bo, PENG Jin-xiu, WANG Zi-ming. Selective flotation of galena from sphalerite using a combination of $KMnO_4$ and carboxylated chitosan [J]. Applied Surface Science, 2022, 602: 154412.

[18] FENG Jin-chan, YANG Bing-qiao, ZHU Huan-yu, ZHANG Han-quan, ZENG Meng-yuan. The utilization of 2-phosphonobutane-1,2,4-tricarboxylic acid (PBTCA) as a novel sphalerite depressant in the selective flotation of galena from sphalerite [J]. Applied Surface Science, 2021, 569: 150950.

[19] LING Yun-jia, CHEN Jun, MIN Fan-fei, CHENG Ya-li, CHU Xin-xia, SHANG Huan-huan, WANG Tian-yue, Influence mechanism of Fe(II/III) doping on the adsorption of methylamine salts on kaolinite surfaces elucidated through DFT calculations [J]. Journal of Molecular Liquids, 2023, 390: 123082.

[20] CHEN Jun, SUN Yu, LING Yun-jia, CHU Xin-xia, CHENG Ya-li, MIN Fan-fei. Effects of Mg(II) doping amount on the surface hydration of kaolinite: Molecular dynamics simulations and experiments [J]. Surfaces and Interfaces, 2024, 45: 103869.

[21] LIAO You-peng, ZHAO Guan-fei, FENG Bo, YAN Hua-shan, WU Hong-qiang, HU Wen-ying, ZHU Dong-mei, QIU Ting-sheng. Application of ultrasonic pre-treatment for flotation separation pyrrhotite from chlorite [J]. Colloids and Surfaces A: Physicochemical and Engineering Aspects, 2023, 669: 131507.

[22] CHEN Ye, TANG Xiao-qin, CHEN Jian-hua, LIU Meng, DFT study of sulfidization mechanism of cerussite ($PbCO_3$) and smithsonite ($ZnCO_3$) [J]. Transactions of Nonferrous Metals Society of China, 2024, 34: 2328−2341.

[23] DAVID S P, MIRIAM M, RAQUEL C J, JOSE M M, OSCAR G, JAVIER R F, JUAN A S, DANIEL E, JOSE M R. Compression of silver sulfide: X-ray diffraction measurements and total-energy calculations [J]. Inorganic Chemistry, 2012, 51(9): 5289−5298.

[24] ZENG Yong, LIU Jian, WANG Yu, LUO De-qiang. Research progress on the interaction mechanism of typical metal ions with sphalerite and its effect on flotation [J]. Conservation and Utilization of Mineral Resources, 2019, 39(2): 109−117. (in Chinese)

[25] LIU Xiao-mei, CHEN Ye, FENG Yao, CHEN Jian-hua. The First-principle study of silver activation and xanthate adsorption on sphalerite surface [J]. Conservation and Utilization of Mineral Resources, 2021, 41(2): 7−12. (in Chinese)

[26] MIAO Yu-qi, ZHAO Guan-fei, FANG Xi-hui, YAN Hua-shan, QIU Xian-hui, YANG Chang-long, ZHANG Shi-ren, QIU Ting-sheng. Investigation the effect of filling materials

on chalcopyrite flotation [J]. Powder Technology, 2024, 431: 119049.
[27] ZHAO Guan-fei, FENG Bo, ZHU Dong-mei, QIU Xian-hui, GAO Zhi-yong, YAN Hua-shan, LAI Rui-seng, QIU Ting-sheng. Enhanced separation of scheelite and calcite by metal-inorganic complex depressant [J]. Transactions of Nonferrous Metals Society of China, 2024, 34: 643−654.
[28] LAN Sheng-zong, SHEN Pei-lun, ZHENG Qi-fang, QIAO Li-dong, DONG Liu-yang, LIU Dian-wen. Effective flotation separation of apatite from dolomite using a new eco-friendly depressant gallic acid [J]. Green Chemisty, 2024, 26: 1627−1636.
[29] LIU Jian-ying, FENG Bo, GUO Wei, CHEN Yuan-gan. Utilizing H_2O_2 for the selective flotation separation of chalcopyrite and galena with their surface pre-adsorbed with Isopropyl Ethyl Thiocarbamate [J]. Separation and Purification Technology, 2024, 330: 125477.
[30] TAN Xin, ZHU Yang-ge, SUN Chuan-rao, XIAO Qiao-bin. Influence of the addition orders of zinc sulfate on adsorption of DDTC in the surfaces of galena & sphalerite [J]. Non-ferrous Metals Engineering, 2022, 12(12): 73−83. (in Chinese)
[31] CHENG Li-li, LI A-lin, HE Yong, ZHANG Zi-wen. The electrochemical mechanism and flotation behavior of galena in ammonium butyldithiOphosphate solution [J]. China Mining Magazine, 2013, 22(12): 113−116. (in Chinese)
[32] HENG J Y Y, ALEXANDER B, ADAM F L, KAREN W, DARYL R W. Anisotropic surface energetics and wettability of macroscopic form I paracetamol crystals [J]. Langmuir: The ACS journal of surfaces and colloids, 2006, 22(6): 2760−2769.
[33] CHAU T T. A review of techniques for measurement of contact angles and their applicability on mineral surfaces [J]. Minerals Engineering, 2008, 22(3): 213−219.
[34] GAO Zhi-yong, JIANG Zhe-yi, SUN Wei, GAO Yue-sheng, Typical roles of metal ions in mineral flotation: A review [J]. Transactions of Nonferrous Metals Society of China, 2021, 31: 2081−2101.
[35] SONG Bao-xu, QIU Xian-yang, RAN Jin-cheng, HU Zhen, LI Pei-lun, YAO Yan-qing. Behavior of argentite in the sulphide flotation system [J]. Precious Metals, 2015, 39(2): 24−28. (in Chinese)
[36] HU Yue-hua, WU Mei-rong, LIU Run-qing, SUN Wei. A review on the electrochemistry of galena flotation [J]. Minerals Engineering, 2020， 150: 106272.
[37] DENG Wen, ZHAN Yun, YU Xin-cai, CAO Yang, LIU Rui-zeng, SHEN Pei-lun, LIU Dian-wen. Study on secondary recovery of lead and zinc from a sulfur concentrate in Yunnan Province [J]. Non-ferrous Metals Science and Engineering, 2023, 14(2): 264−271. (in Chinese)
[38] WANG Han, WEN Shu-ming, HAN Guang, FENG Qi-cheng. Effect of copper ions on surface properties of $ZnSO_4$-depressed sphalerite and its response to flotation [J]. Separation and Purification Technology, 2019, 228: 115756.
[39] HENG Yu, ZHANG Hong-liang, ZHANG Chen-yang, SUN Wei, HAN Ming-jun, WANG Rong, WEI Xin, LI Song-jiang, Adsorption characteristics of Ag^+ on sphalerite surface: A combined experimental and first-principle study [J]. Environmental Science and Pollution Research International, 2024, 31: 23822−23828.

矿浆中银离子和锌离子共存时辉银矿和闪锌矿表面丁铵黑药的吸附特性

邱廷省[1,2]，丁开伟[1,2]，赵冠飞[1,2]，李国栋[1,3]，杨雯慧[1,2]，程 浩[1,2]，颜顺德[1,2]

1. 江西理工大学 战略金属矿产资源低碳加工与利用江西省重点实验室，赣州 341000；
2. 江西理工大学 资源与环境工程学院，赣州 341000；
3. 西北矿冶研究院，白银 730900

摘 要：研究了丁铵黑药(ADD)对辉银矿和闪锌矿的浮选分离。分子模拟(MS)计算表明，ADD 以 S—P 键的形式化学吸附在辉银矿和闪锌矿表面。ICP、Zeta 电位和 XPS 分析揭示了 Ag^+体系中 ADD 在辉银矿和闪锌矿表面的吸附特性。结果表明，辉银矿表面溶解的 Ag^+可以以氢氧化银的形式吸附在闪锌矿表面，而 AgOH 亲水性胶体阻止 ADD 在闪锌矿表面的吸附。吸附量和表面润湿性分析揭示了矿浆中银离子和锌离子共存时 ADD 在辉银矿和闪锌矿表面的吸附特性。结果表明，$Zn(OH)_2$ 和 AgOH 亲水性胶体的组合使得辉银矿表面 ADD 吸附量和疏水性相对于闪锌矿更强。浮选试验表明，矿浆中银离子和锌离子共存时 ADD 能够有效分离辉银矿和闪锌矿。

关键词：辉银矿；闪锌矿；丁铵黑药；银离子；吸附

(Edited by Bing YANG)